

Understanding ice accretion on wind turbines with field data

Patrice Roberge¹, Jean Lemay¹, Jean Ruel¹, André Bégin-Drolet¹

¹ Université Laval, Québec, Canada

Patrice.Roberge.2@ulaval.ca, Jean.Lemay@VRRH.ulaval.ca, Jean.Ruel@gmc.ulaval.ca, Andre.Begin-Drolet@gmc.ulaval.ca

Abstract— With the abundance of wind resources in cold climates, a significant share of the worldwide wind energy installed capacity is located in those areas. However, the advantages of cold climate operation comes with challenges associated with ice accretion. Throughout the years, alternative operational strategies have been developed to cope with these challenges. Although many strategies, such as blade heating, have been commercially available for a long time, few field studies have investigated their performance. Evaluating the performance of wind turbines in cold climates is a hard task due to the lack standards and the variability of external factors influencing turbine behaviour. In this paper, a methodology to assess the performance of wind turbines in cold climates is illustrated with a case study. This methodology aims to provide a better understanding of how ice accretion impacts wind turbine performance. With this knowledge, the design of alternative operational strategies can be improved.

Keywords— Wind turbine, meteorological icing, field data, wind energy, meteorological measurements.

I. INTRODUCTION

Ice accretion has been an issue for wind energy production in cold climates since its beginning. Concerted efforts to tackle this challenge date back to the first BOREAS conference in 1992. Through the sharing of operational experience and the knowledge gained with experimental tests, the wind energy production in cold climates significantly evolved through the years. However, the private nature of wind energy in many countries slowed down the sharing of field test results and subsequently the understanding of how icing impacts wind turbines [1]. Researchers thrived on new numerical resources to better model ice accretion, but few of them actually applied their results to real-life situations [2].

Through partnerships with wind farm owners and third parties, we had the opportunity to install ice sensors and cameras on the nacelle of several wind turbines. Additionally, we had access to the production data of a large number of wind turbines installed in cold climates. With state-of-the-art technology installed on-site, it was possible to enhance the understanding of how ice accretion impacts the energy production of wind turbines.

Recently, scientists, third parties and wind turbine manufacturers have developed new alternative operational strategies (AOS) such as retro-fit ice protection systems (IPS) and active modification of the tip speed ratio during icing events [3]. The usage and the evaluation of such strategies require a complete understanding of the physics of icing on wind turbines. There are currently no widely accepted standards on how to assess the performance of AOS adapted to the reality of field data [4]. The main challenge is that icing is a complex phenomenon and that there are many factors that can influence the performance of a wind turbine [5].

The first step in the analysis of the performance of wind turbines in cold climates is to develop an appropriate methodology to select relevant data. Since there is a lot of data available, selecting the right information and maximizing its usage proves to be the main challenge. There are three main types of data that are relevant to this analysis: turbine data (*e.g.* power, rpm and status codes), meteorological data (*e.g.* wind speed, temperature and icing data) and IPS data (*e.g.* activation and status). The turbine status codes are particularly important since they allow to identify instances where the turbine is not in normal operation (*i.e.* maintenance, icing or forced outage). They become useful later in the analysis to exclude external factors from the results. Unfortunately, their format varies depending on the turbine type and the operator. Few turbines are equipped with ice sensors [6] and it is therefore not possible to fully understand the behaviour of the turbines and their IPS.

The second step consists of defining tools to increase the value of the data. For example, a common practice in the wind industry is to use a power curve to estimate the available power from the wind speed [6]. Using the manufacturers power curve can prove to be inaccurate as it has been calibrated under ideal conditions (*e.g.* flat terrain, limited turbulence intensity, etc.) [7]. Thus, using field data to define empirical power curves for each turbine provides a more accurate way to estimate the available power based on the wind speed and other meteorological parameters such as the ambient temperature [8]. However, to generate these power curves, it is necessary to generate a data set including only the periods where the turbine is in normal operation. This can prove to be a difficult task since the turbine performance can be affected by several factors such as ice accretion on the blades [1]. Completely filtering those occurrences from the dataset is not trivial and requires advanced numerical tools and algorithms.

Since icing conditions vary significantly from one year to another [9], it is not possible to use the turbine itself as a baseline. To adequately assess the performance of an AOS, it is necessary to identify nearby turbines for comparison purposes. These turbines, also referred as control turbines, should not be using the AOS. Even though the wind and icing conditions vary within a wind farm, if the turbines used for comparison are chosen wisely, it is possible to get an accurate outlook on the performance of the AOS [10].

To numerically describe the performance of the AOS different metrics have been developed. Since every turbine is experiencing different wind conditions, it is important that the metrics compensate for any biases that may arise from these differences [4].

Once all these tools are put in place, it is possible to assess the impact of ice accretion on wind turbines behaviour and understand how the AOS performed under those conditions.

In this paper, the steps described above are illustrated by a case study. From the selection of the data to the interpretation of the impact of icing on a four-turbine cluster during a nine-day icing event. The methodology is exemplified using field data.

This case study provides an example on how to integrate the different information (*e.g.* meteorological measurements and turbine performance data) to draw conclusions regarding the AOS performance. This methodology will help wind farm owners to evaluate the profitability of AOS in trial situations before deploying the strategy to the rest of the wind farm. It will also help to better understand how ice accretion affects the performance of wind turbines.

II. METHODOLOGY

As mentioned previously, the method is detailed in four separate steps: data selection, analysis tools, selection of the control turbines, and the interpretation of the icing event.

A. Data selection

The data used in the case study was retrieved from an undisclosed wind farm located in eastern Canada. The wind farm has been estimated to be an IEA ice class 4. Initially, the turbines on this site were not equipped with an IPS and some of them were retrofitted with a hot-air IPS as an AOS. For confidentiality purposes, the active power of the turbines has been scaled to 3MW to preserve data anonymity. The turbine equipped with the IPS was defined as the experimental turbine.

This turbine was equipped with an ice sensor, the Meteorological Conditions Monitoring Station (MCMS), to provide valuable information regarding the meteorological icing status. The MCMS comprises two patented heated probes [11], an ultrasonic anemometer, a humidity sensor, a barometric pressure transducer, an ambient temperature sensor and a solar radiation sensor. By combining the power drawn by the heated probes as well as the surface temperature of these probes and the wind speed and ambient temperature, it is possible to detect liquid water particles colliding with the probe surface. The increase of the heat transfer due to the presence of liquid water particles on the heated probe surface can be used to estimate the icing severity defined as the droplet impingement flux to the surface of the probe [12].

The example presented in this paper is composed of an experimental turbine and 7 turbines that are not equipped with the AOS. The data used in this paper was retrieved from the Supervisory control and data acquisition (SCADA) system, from the MCMS, and from the IPS controller.

B. Analysis tools

To assess the performance of a wind turbine, the available power based on the ambient conditions needs to be estimated. This task is usually done using a power curve which links the nacelle measured wind speed to the power generated by the turbine in normal operation. To generate a power curve it is crucial to remove any data points observed when the turbine power output is affected by any other parameter (*i.e.* maintenance, stoppage, curtailment or ice accretion). The maintenance and curtailment events can easily be removed when reliable turbine status codes are provided. Different

strategies have been used in the past to remove the data points associated with rotor icing and in this study, it was decided to use the icing event finder algorithm presented in Roberge *et al.*[8]. This algorithm uses the combination of individual performances of wind turbines within a cluster.

As defined by the International standard IEC 61400-12-1 [13], the wind speed and power were averaged for each bin corresponding to wind speed intervals of 0.5 m/s. The power curve was modelled by a piecewise function as defined in Eq. 1 where u is the wind speed and $P(u)$ is the power curve function. The first part of the equation yields a power equal to 0 for wind speeds below the cut-in wind speed (u_{ci}). The second part of the equation is a fifth order polynomial fitted between the cut-in and rated (u_r) wind speeds. Finally, for wind speeds above the rated value, the power curve function is equal to the rated power (P_r). The cut-in and rated wind speeds can either be taken from the manufacturer or deduced from the data. Generating individual power curves for each turbine yields significantly more precise estimations of the available power.

$$P(u) = \begin{cases} 0 & \text{if } u < u_{ci} \\ P_5(u) & \text{if } u_{ci} < u < u_r \\ P_r & \text{if } u > u_r \end{cases} \quad (1)$$

To accurately identify periods where the turbine is producing less power than expected, it is necessary to define a power curve threshold. A threshold based on a percentage of the actual power curve is not sensitive enough for high wind speeds. Thresholds based on the standard deviation of quantile values of each previously defined bins yielded better results but require to carry a large amount of additional information for each turbine. As proposed in Roberge *et al.* [8], it is possible to achieve a similar accuracy with a threshold ($P_{thstd}(u)$) based on the power curve as defined in Eq. 2 where s_1 and s_2 are two sensitivity parameters. In this study, a s_1 of 0.25 m/s and a s_2 of 75 kW were used.

$$P_{thstd}(u) = P(u) - (P(u - s_1) - s_2) \quad (2)$$

Once the threshold has been set, the periods where the turbine was experiencing power losses due to icing can be identified. Knowing that data points influenced by rotor icing are usually contiguous, it is possible to use that temporal dependency to define Significant Production Loss (SPL) periods. Considering only the icing losses during these periods helps to make the assessment of icing losses more accurately. In this paper, the algorithm described in Roberge *et al.* [8] was used to identify SPL periods.

C. Selection of control turbines

To assess the effect of using an AOS, it is necessary to compare the turbine behaviour to neighbouring turbines rather than the performance of the turbine in previous years, since large inter-annual variations are often observed. To improve the confidence in the results, it was decided to choose three turbines to compare to the experimental turbine, defined as control turbines. Having three control turbines is particularly useful when some turbines are stopped for maintenance during icing events. It also helps to reduce the impact of stochastic

events such as ice shedding. Correctly selecting comparable control turbines is a vital part in achieving accurate results since wind and icing conditions may significantly vary within a wind farm. Not choosing representative control turbines could induce a bias in the results.

The selection of control turbines must be made over a period where every turbine, including the experimental turbine, is operating without the AOS. This period was divided into two data sets: one ice-free and the other only including the icing events. Both data sets excluded stoppages not related to icing. The correlation coefficient between the power generated by the experimental and each potential control turbine was computed for the ice-free (ρ_{if}) and ice (ρ_i) data sets. An overall grade was awarded to each potential pairing using Eq.3.

$$Score = 0.6\rho_{if}^2 + 0.4\rho_i^2 \quad (3)$$

As an additional criterion, the energy efficiency metric (η), defined in section II.C. was computed for the icing event data set. The following set of rules was then applied based on the number of turbines with a grade within 10% (n_{10}) and 5% (n_5) of the top grade:

- $n_{10}=3$: Select the turbines with the three best scores.
- $n_{10}<3$: The process has to be done manually (consider using only two control turbines).
- $n_{10}>3$: Use the following rules:
 - $n_5=1$: Select the combination of the turbine with the best score and two turbines included in n_{10} that yields an average energy efficiency (η) in the icing event data set closer to the value of the experimental turbine.
 - $n_5=2$: Select the combination of the two turbines with the best scores and one turbine included in n_{10} that yields an average energy efficiency (η) in the icing event data set closer to the value of the experimental turbine.
 - $n_5=3$: Select the three turbines with the best scores.

In every case, it is important to pay attention to the average value of the energy efficiency metric of the three control turbines. This value determines whether there is a bias due to harsher or milder icing conditions.

D. Interpretation of an icing event

With three control turbines selected for the experimental turbine, the performance of the turbine equipped with the AOS can be evaluated using three metrics: the energy efficiency metric, the energy gain metric and the potential recovery metric.

1) *Energy Efficiency metric*: The energy efficiency metric is defined as the produced energy (E_{prod}) over the available energy (E_{avail}) during a certain period as defined in Eq. 4. The available energy was obtained by integrating the available power from the power curve model during this period.

$$\eta = \frac{E_{prod}}{E_{avail}} \quad (4)$$

This metric has the advantage of being easy to compute and compare. However, the metric is dependent on the period selection and on the available energy. For example, a turbine with a higher available power during icing stoppages is more heavily penalized compared to another turbine with exactly the same stoppage time.

This metric can be improved by using the energy losses computed only during SPL periods (E_{loss}) as defined in Eq. 5 where P_{prod} is the produced power, P_{avail} is the available power obtained from the power curve and dt^* represents the timestamps interval where SPL were detected. The energy efficiency can then be computed using Eq. 6.

$$E_{loss} = \int (P_{avail} - P_{prod})dt^* \quad (5)$$

$$\eta = \frac{E_{avail} - E_{loss}}{E_{avail}} \quad (6)$$

2) *Energy Gain Metric*: The energy gain metric is defined as the amount of extra energy the experimental turbine produced because of the usage of the AOS based on the performance of a control turbine. To compute this metric, it is necessary to evaluate the power efficiency (PE) of the experimental and control turbines at each timestamp as defined in Eq.7

$$PE = \frac{P_{prod}}{P_{avail}} \quad (7)$$

The energy gain metric of an experimental turbine compared to a control turbine ($Gain_{ex-ct}$) is then obtained by integrating the difference between the power efficiency of the experimental turbine (PE_{ex}) and of the control turbine (PE_{ct}) multiplied by the available power of the experimental turbine ($P_{avail-ex}$) over the periods where SPL were detected on either of the turbines (dt^*) as defined in Eq. 8.

$$Gain_{ex-ct} = \int (PE_{ex} - PE_{ct})P_{avail-ex}dt^* \quad (8)$$

While being more complex than the energy efficiency metric, the energy gain metric is significantly less sensitive to the selection of the period and to the difference in the available power.

3) *Potential Recovery Metric*: The potential recovery metric is defined as the percentage of the losses experienced by the control turbine that could have been recovered if it was using the AOS of the experimental turbine. The potential recovery was evaluated using Eq. 9 where $E_{Loss-ct}$ is the energy loss of the control turbine. It is important to note that in this equation the indexes of the energy gain have been swapped. This modification means that the available power of the control turbine is used instead of the one of the experimental turbines in Eq. 8.

$$PR_{ex-ct} = \frac{-Gain_{ct-ex}}{E_{Loss-ct}} \quad (9)$$

III. RESULTS

A. Analysis tools

For each turbine of the cluster, icing events were identified and a data set without maintenance or icing was generated. Using the methodology presented in section II.B. power curve functions were generated. Fig. 1 presents an example of a data set, binned averages and the power curve function.

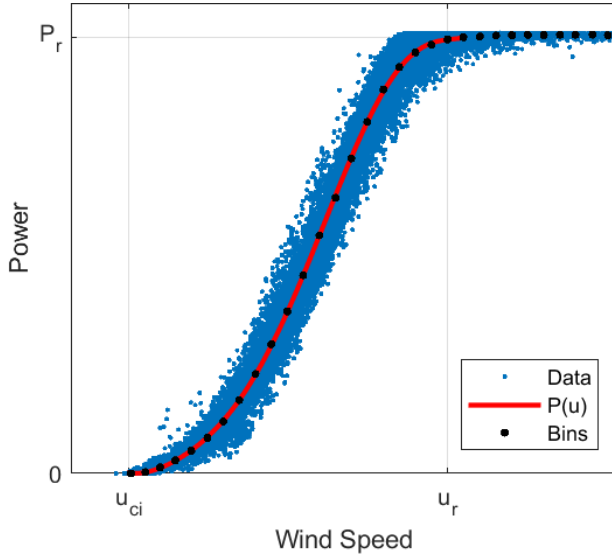


Fig. 1: Power curve of one of the turbines of the cluster. The filtered data to only keep out points not associated with icing or maintenance are shown in blue. The different bins are shown in black and the power curve ($P(u)$) is shown in red. To preserve data anonymity, the axes were limited to the cut-in wind speed (u_{ci}), the rated wind speed (u_r) and the rated power (P_r).

B. Selection of the control turbines

With a complete data set of 397 days with the 8 wind turbines comprised in the cluster were operating without the AOS. This data set was then divided into a data set excluding icing events (clean) and including icing events (ice). The icing data set comprised a total of 93 days. For every potential control turbine labelled from A to G, the correlation coefficient squared between the produced power of the experimental and control turbine was evaluated. The energy efficiency metric for the ice data set was computed for every turbine in the cluster. The correlation coefficients, the corresponding score from Eq. 3 and the energy efficiency metrics are presented in Table I. With the rules described in Section II.C., it is possible to determine that the three best suited control turbines were B, E and F.

TABLE I: CONTROL TURBINE SELECTION DATA

	Clean R^2 [%]	Ice R^2 [%]	Score [%]	η_{ice} [%]
Exp.	-	-	-	43
A	72.4	67.7	70.5	38
B	89.7	85.2	87.9	44
C	77.5	74.9	76.5	41
D	74.8	70.4	73.1	37
E	81.0	77.1	79.5	44
F	80.9	76.2	79.0	43
G	74.6	63.6	70.2	38

C. Interpretation of an icing event

In this section, a 9-day icing event was used as a case study to demonstrate how field data can be used to enhance the analysis of AOS. To fully understand the context of the icing event, it is necessary to start with an overview of the icing conditions as presented in Fig. 2. In this figure are represented several of the MCMS measurements: nacelle wind speed, ambient temperature measured from the nacelle, solar factor, relative humidity and icing severity.

It is possible to observe that this event did not feature wind speeds below 5 m/s. This observation is not surprising, since icing events are generally associated with strong winds. It is also observed that on the 5th day, the wind speed surpasses 25m/s, approximately the cut-out value of the turbine.

The ambient temperature measured from the nacelle varied between -29 and -4°C throughout the icing event. The solar factor was defined as the ratio of the solar radiation measured on the nacelle and the expected value for a clear sky based on the position of the sun at that specific time. It is possible to observe that the solar factor seldom rises over 50% during the icing event. The only moments where the solar factor reaches 50% are on the 5th and 6th day and on both occasions, significant variations in the value were observed in a short amount of time. This behaviour might be explained by low clouds periodically passing through.

The relative humidity stayed above 80% during the event except for a period between the 87th and 100th hour of the event. For most of this icing event, the conditions were favourable for ice accretion and the extent of sublimation of the ice accreted on the surfaces was limited by the high relative humidity.

Meteorological icing can be inferred with non-null icing severity values. Three main icing episodes can be observed. The first icing episode started at the 15th hour and ended at the 40th hour. The second icing episode occurred between the 100th and 144th hour. The last icing episode was observed between 155th and 180th hour.

The first icing episode featured high icing severities and ended with a sharp increase in wind speed and a sharp decline in temperature.

The second icing episode started with an abrupt rise of the relative humidity. The wind speed went above 25 m/s during this event resulting in high icing severity values. Shortly after the wind speed stabilized at 15 m/s, the temperature peaked

just before the 120th hour at -4°C. For the second half of the episode, the temperature gradually went down to -20°C as the icing severity was reduced.

During the third icing episode, the temperature rose to -5°C as the winds remained stable between 10 and 15 m/s. The maximal icing severity reached was lower compared to the other icing episodes.

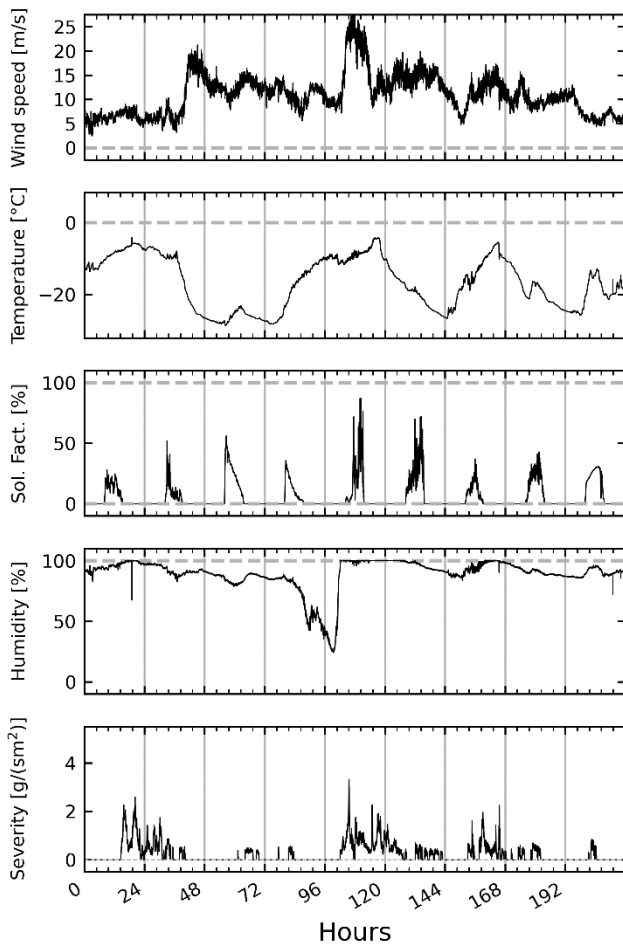


Fig. 2: Meteorological measurements made by the MCMS during the 9-day icing event.

The time series of the power production of the experimental turbine and the three selected controls are presented in Fig. 3. In this figure, the information is layered in three levels. The status code ribbon on top of each subplot where the relevant information regarding the status of the turbine is displayed. The relevant status codes are: reduced production or stoppage due to icing (icing), stoppage not related to icing which can be a forced outage or a maintenance (other stop), tower oscillation related status codes (tower) and normal operation status code (OK). The second level of information is the middle plot where the power generated by the turbine is presented in black and the available power estimated with the power curve is presented in red. Blue and red zones are superposed to these values to represent respectively the detection of meteorological icing by the MCMS (MI) and the activation of the blade heating IPS (BH). It is important to note that meteorological icing can be observed while the IPS is active, resulting in a purple zone. The third and final level of

each subplot is used to display the SPL periods portrayed by the yellow zones.

During the first icing episode, it is possible to observe that, even though the IPS was active, the turbine was not able to generate power. Shortly after the end of the detection of meteorological icing, the experimental turbine was able to produce at or close to the expected power while the three control turbines remained stopped. This observation is coherent with the fact that the operational envelope, the ambient conditions for which the IPS is expected to be efficient, may be dependent on the icing severity. At the 48th hour, the power produced by the experimental turbine dropped to 2000 kW even though no new ice was detected. This reduction coincided with the average wind speed going from approximately 18 m/s to 12 m/s which was still above the rated wind speed. It is a good example where wind speeds over the rated value can mask the impact ice accretion impact on power production. When the turbine reaches the rated power, the blades pitch is decreased to maintain the rated power. With a smaller angle of attack and more energy available, the turbine may be able to produce at its rated power even with ice accreted on the blades. The behaviour of the turbine at the 48th hour is a good example of this effect where the impact of ice accretion reappears as the wind drops. With the low temperature observed for most of this event, the efficiency of the IPS was limited. As the event progresses, at around the 80th hour, the turbine was able to regain full power. A couple of hours later, control turbine 1 and 2 restarted. Control turbine 3 remained stopped due to a forced outage unrelated to icing. It is important to exclude from the analysis, the period where the turbine was stopped for reasons unrelated to icing, otherwise the analysis would be biased.

The second icing episode starts with the wind speed going over the cut-out value causing the experimental turbine and control turbine 1 to stop for short amount of time. This time, the IPS was able to minimize the losses associated to icing. The temperature got up to 4°C before rapidly dropping under -20°C. This observation stresses the importance of a timely activation of the IPS, since the efficiency of the system in the latter half of the episode was probably limited. The control turbines had to wait until the 150th hour to fully recover from the icing episode.

The third icing episode was less intense in terms of icing severity but the accretion phase occurred with slightly lower temperatures. Ice shape and density are strongly dependent on the ambient temperature and they, in turn, have a different aerodynamic impact on the blades. It is possible to observe that the third icing episode had a major impact on the performance of the four turbines. As the temperature decreased past the 168th hour, the efficiency of the IPS became limited. However, the experimental turbine still clearly outperformed the three control turbines. The experimental turbine fully recovered from the icing event around the 200th hour as the temperature rose again. The control turbines only fully recovered by the very end of the event.

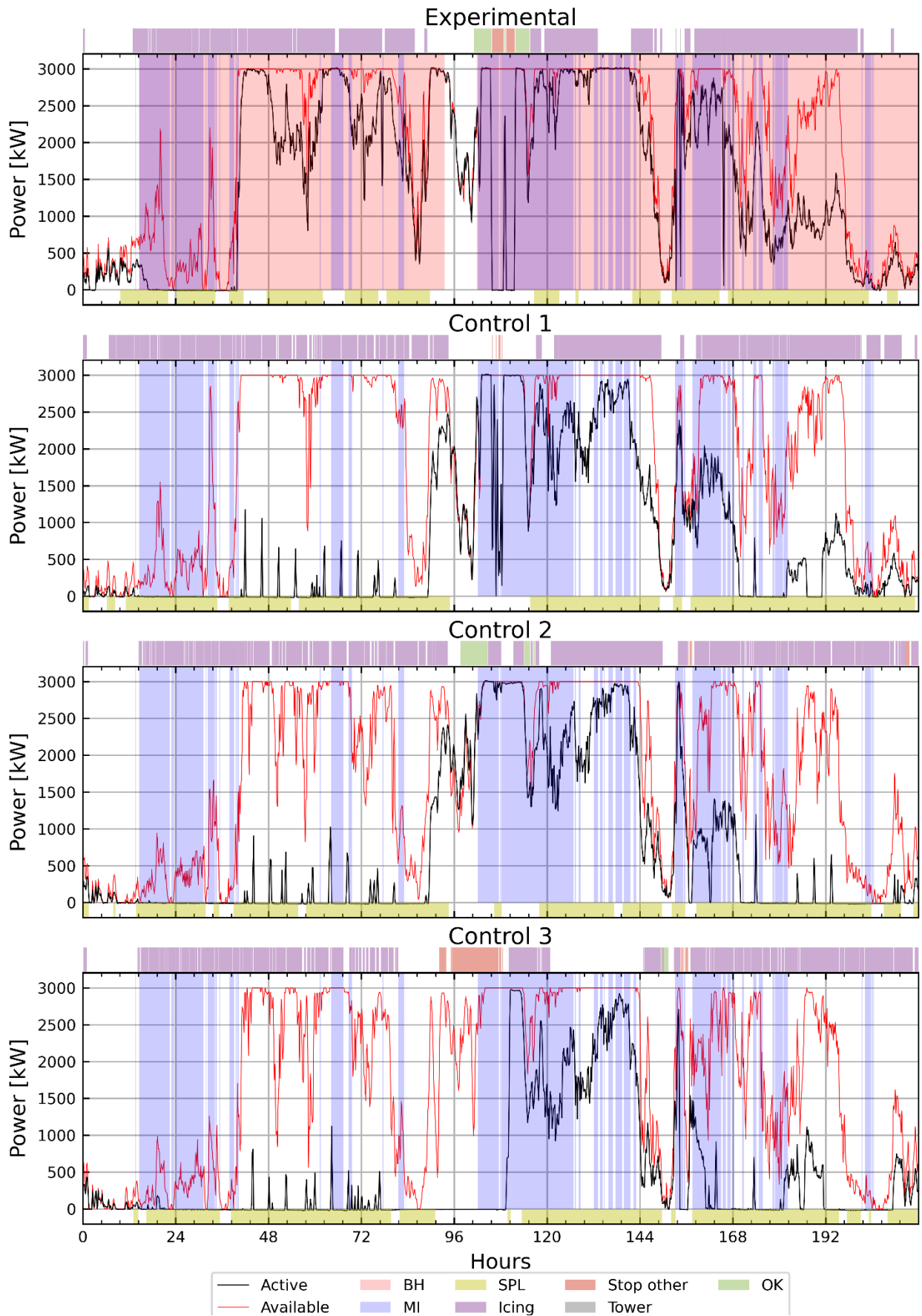


Fig. 3: Time series analysis of the performance of the experimental turbine (equipped with an IPS) and three control turbines (unheated). This figure highlights the active and available power generated for each turbine, the meteorological icing (MI) detection and blade heating (BH) periods. Each subplot is supported by a turbine status code detailing icing, turbine stoppage unrelated to icing (stop other), tower oscillation (tower) and normal operation (OK).

TABLE II : COMPARISON OF THE PERFORMANCE OF THE EXPERIMENTAL TURBINE (EXP.) TO THE THREE CONTROL TURBINES (C.1, C.2 AND C.3) DURING THE 9-DAY ICING EVENT.

Turbine	Efficiency [%]	Available [MWh]	Produced [MWh]	Loss [MWh]	Gain [MWh]	Recovery [%]	IPS cost [MWh]
Exp.	79	429	330	90	-	-	15
C.1	42	417	164	244	152	60	-
C.2	43	389	158	221	159	63	-
C.3	33	340	95	227	166	63	-

To complement the visual analysis provided by the time series, the metrics defined earlier were computed for this event and are presented in Table II. As expected the energy efficiency metric of the experimental turbine is significantly higher compared to the control turbines (79% vs. 42%, 43% and 33%). It is important to note that there is a notable difference in the available energy of the different turbines. Control turbine 3 had a significantly lower available energy since the period where it was stopped due to a reason not related to icing was removed from the calculation. Only the energy gain and potential recovery metrics were computed on common periods as the experimental turbine. The icing losses of the control turbines are significantly greater than the ones of the experimental turbine. The energy gain metric reveals that the operation of the IPS was very profitable as gains between \$15k and \$17k were observed (assuming a selling price of \$0.10/kWh). Potential recovery metrics between 60 and 63% were computed indicating that the IPS negated most of the icing losses during this icing event. The meteorological conditions at the start of the first icing episode and the end of the third episode did not allow the IPS to be fully effective, therefore limiting the potential recovery metric. In this icing event, the IPS was using a very sensitive trigger strategy and thus was active for most of the event. Even with this aggressive triggering strategy, the heating costs accounted for less than 10% of the energy gains.

IV. CONCLUSIONS

In this paper, a methodology for assessing the performance of wind turbines in cold climates was proposed and demonstrated via a case study. The case study covered the process of data selection, generation of power curves, selection of control turbines and interpretation of icing events.

With the right numerical tools it is possible to accurately estimate the available energy and therefore the extent of icing losses. The more efficient way to evaluate the performance of an AOS is to compare the turbine behaviour to the one of a nearby turbine with similar conditions. The selection of the turbines used for comparison must balance out the similarity in winds and the similarity in icing conditions. In this study, the selection process was exemplified with a data set of one experimental turbine and 7 potential control turbines. With the use of the correlation coefficients between their power produced inside and outside of icing events as well as their performances during icing events, the three best suited turbines were selected.

Finally, with the different tools set and the control turbines selected, an analysis example of an icing event was presented.

This case-study integrated the turbine, meteorological and IPS data. The different portions of the field data helped to paint a full picture of the icing event. The meteorological data helped to understand, time-wise, what conditions are favourable to the IPS efficiency. It also allowed to quantify the effect of the AOS on the turbine performance. In this icing event, the retrofit hot-air IPS yielded an average energy gain of 159 MWh and an average potential recovery of 62%. The interpretation of the icing event allowed to observe the masking effect that high winds can have on rotor icing. It also helped to observe the effect that temperature has on the ice accretion and shedding. In the accretion phase, the temperature will determine the ice shape that also determines its aerodynamic impact.

This methodology helps to better understand icing events, which opens the door to the optimization of energy production with the use of AOS. These strategies are often designed numerically or in laboratories and few of them have been validated in real-life conditions. The case-study presented in this paper was limited to the installation of a retrofit IPS as the AOS, but this methodology could also be used to understand the performance of other AOS such as: control strategies (*e.g.* reduced TSR and pitch reduction modes), passive IPS (*e.g.* ice-phobic coating) or a different triggering strategy for active IPS.

ACKNOWLEDGMENT

The authors would like to gratefully acknowledge the Natural Sciences and Engineering Research Council of Canada (NSERC) (RGPIN-2015-04564, EGP-542652-19, ALLRP-556945-20 and BESD3-54761-2020) for the financial support they provided for this research. The authors would also like to acknowledge the openness and the active participation of their industrial partners for giving us the opportunity to use their data in this research.

REFERENCES

- [1] Z. Canovas Lotthagenm "Defining, analyzing and determining power losses-due to icing on wind turbine blades", Masters degree, Malardalen University, Sweden, 2020.
- [2] L. Gao, T. Tao, Y. Liu, and H. Hu "A field study of ice accretion and its effects on the power production of utility-scale wind turbines" *Renewable Energy*, 167, 917-928, Apr 2021.
- [3] C. Godreau, H. Wickman, T. Karlsson, S. Soderberg "Performance Warranty Guidelines for Wind Turbines in Icing Climates" IEA Wind TCP Task 19 Technical Report, Sep 2020.
- [4] P. Roberge, D. Baxter, J. Ruel, D. Roeper, J. Lemay, and A. Bégin-Drolet, "Towards standards in the analysis of wind turbines operating in cold climate. Part B: Methodology for evaluating wind turbine

- alternative operational strategies”, *Cold Regions Science and Technology*, 103494, Jan 2022.
- [5] R.E. Bredesen, R. Cattin, N.-E. Clausen, N. Davis, P.J. Jordaens, Z. Khadiri-Yazami, R. Klintström, A. Krenn, V. Lehtomäki, G. Ronsten, M. Wadham-Gagnon, and H. Wickman, “IEA Wind TCP Recommended Practice 13 2nd Edition: Wind Energy in Cold Climates: IEA”, 2017.
- [6] S. Hildebrandt, “Modeling and evaluation of wind turbine operational strategies during icing events”, Master's thesis, Schulich School of Engineering, 2019.
- [7] L.T. Paiva, C. Veiga Rodrigues, and J.M.L.M. Palma, “Determining wind turbine power curves based on operating conditions”, *Wind Energy*, 17(10), 1563-1575, 2014.
- [8] P. Roberge, J., Lemay, J. Ruel, and A. Bégin-Drolet, “Towards standards in the analysis of wind turbines operating in cold climate–Part A: Power curve modeling and rotor icing detection”. *Cold Regions Science and Technology*, 103436, 2021.
- [9] J. Hansson, J. Lindvall, and Ø. Byrkjedal, “Quantification of icing losses in wind farms” Kjeller Vindteknikk, Stockholm, Sweden, Report, 299, 2016.
- [10] C. Godreau, H. Wickman, T. Karlsson, and S. Soderberg, “Performance Warranty Guidelines for Wind Turbines in Icing Climates” IEA Wind TCP Task 19 Technical Report, Sep 2020.
- [11] A. Bégin-Drolet, J., Ruel, and J. Lemay, “U.S. Patent No. 9,846,261” Washington, DC: U.S. Patent and Trademark Office, 2017.
- [12] P. Roberge, J., Lemay, J. Ruel, and A. Bégin-Drolet, “In situ estimation of effective liquid water content on a wind turbine using a thermal based sensor”, *Cold Regions Science and Technology*, Volume 184, 2021, 103235, ISSN 0165-232X, <https://doi.org/10.1016/j.coldregions.2021.103235>, 2021.
- [13] International standard IEC 61400-12-1, “Wind turbines- Power performance measurement of electricity producing wind turbines”, 2005.